Alcohol Dependence in Mice: A Cocktail of Change in Region-specific mRNA Concentration and Protein Amount

By

Julie Lee

Senior Honors Thesis

Department of Chemistry

University of North Carolina at Chapel Hill

April 27, 2022

Clyde W. Hodge, Thesis Advisor

Jillian L. Dempsey, Committee Chair

Thomas C. Freeman, Committee Member

Table of Contents

ACKNOWLEDGMENTS

Edit: After multiple revisions to this page, I admit that no amount of writing of this length can truly capture the thesis writing and the Hodge lab experience. Maybe, I would have filled more pages if my thesis was about the Hodge Podge instead.

First, I would like to thank my committee members, Dr. Jillian L. Dempsey and Dr. Thomas C. Freeman, for reviewing my thesis and presentation. I have had the privilege to call them my professor or student organization advisor, and am so honored that I got to have these distinguished and well-loved faculty in my thesis committee.

I would also like to shout out my faculty advisor Dr. Clyde W. Hodge, without whom this experience would not have been possible. Dr. Hodge has been a constant advocate for my research endeavors and growth throughout my years at the lab, always setting aside time to advise, listen, and (constantly!) encourage my work, thoughts, and interests. From a culmination of accounts including my own, I know Dr. Hodge's considerations and mentorship towards his lab members are unparalleled. I can attest even from our first email exchange, where he promptly and thoughtfully responded to my cold email.

I would also like to thank Hodge lab members of the past and present, who all made me look forward to coming into the lab. Notably, it was through Michelle Kim, a former lab technician, that I came to know of this great family. But more than in the professional context, I thank Michelle for having been my friend and mentor throughout the earlier, tougher half of my college career. Michelle gets along with everyone, and anyone who gets the chance to meet her has no trouble understanding how. Her gentle demeanor, considerate remarks, meme-y humor, and willingness to go extra miles for others has modeled for me traits I want to embody. In addition, I would like to thank Ciarra Whindleton, who co-parented this project with me. Just like the ideal spouse, Ciarra was always in sync with me to communicate all aspects of this project, not to mention the quickest to encourage me when things went awry. In a short period of time, Ciarra has become my lab confidant and daily dose of witty/sassy exchanges, and I hope to find a work best friend like her wherever I go in the future.

Finally, I want to thank another lab dynamic duo, Dr. Sara Faccidomo and Dr. Jessica Hoffman. This acknowledgement page would never be complete without mentions of either one of them, as they took extended time, effort, and patience to guide each step of my learning. Even through extenuating circumstances and deadlines of their own, they prioritized and made themselves available for my questions, and I owe all of my projects and what I know about research to them. Funny enough, I never called either one of them "Drs"; Jessica always looked out for me like an older sister, ensuring that I ate and slept, making me baked goods and coffee, and providing ample amounts of moral support and bewildering stories to keep me going. In conjunction, her flawless analogies and unofficial role as the lab's troubleshooter exemplified for me that academia takes much more heart and light than just intelligence and grit.

If Jessica was my 24/7 tech support, Sara was my customer support hotline. As my point of contact for all things lab related, Sara exercised great patience, understanding, and empathy to hold my hand to teach me all I know. She never ceased to reply to my emails or Teams messages even at the oddest hours, and never failed to remember and follow up on subtle details of my life. Sara's stories and updates of her family also made injection, decap, and brain punch days fly by quicker, and I do not know who else I can talk about Korean food with when I move elsewhere. In exchange for the headaches I caused her, she surely is going to repay me with heartache as I leave her guidance and grow to realize how much of an imprint she and this lab has had on me. I also thank donors of the Salisbury Family Excellence Fund for making this opportunity possible.

ABSTRACT

Alcohol dependence poses great challenges against addressing Alcohol Use Disorders (AUD) by increasing tolerance to the drug's adverse effects and inducing distressing withdrawal symptoms. With chronic alcohol use, the brain adjusts to recurrent excessive inhibitory signaling through physiological changes to upregulate excitatory neurotransmission. In particular, glutamate-detecting α-amino-3- hydroxy-5-methyl-4-isoxazolepropionic acid receptor (AMPAR) increases in synaptic density and activity upon prolonged alcohol use by an unknown mechanism. The shift towards glutamate signaling is indicative of neuroplasticity and anxiety-like symptoms that favor elevated alcohol drinking patterns. To identify the mechanism as to which dependence develops through the AMPAR pathway, C57BL/6J mice underwent the well-established Chronic Intermittent Ethanol (CIE) exposure to induce physiological responses similar to those observed in alcohol dependence in humans. Then, through qRT-PCR, gene expression of AMPAR pathway components associated with alcohol drinking behavior (GluA1, TARP-γ8, and PSD-95) were observed in brain regions (Prefrontal Cortex, Amygdala, Insular Cortex, and Nucleus Accumbens) particularly sensitive to excitatory signaling and interconnected in the reward pathway. Gene expression changes were then verified with relative protein concentrations to ensure processing of mRNA for activity. Significant changes indicate modulation of components of interest, which project onto the Nucleus Accumbens to retain neural homeostasis. In relation to protein concentration, further experimentation, such as varying decapitation time, is necessary to account for additional cellular and biochemical considerations such as mRNA and protein processing, time in between and during transcription and translation, and reaction with the inter- and intracellular environment. Follow up studies to this experiment will provide clearer insight into molecular targets for pharmacological AUD interventions.

INTRODUCTION

Alcohol Use Disorder (AUD) is the leading cause of preventable death, claiming approximately 95,000 deaths per year in the United States[1]. Alcohol use also worsens existing illnesses and increases the risk of co-morbidity for over 200 diseases and health conditions, including cancer (liver, mouth, breast, throat, esophagus), dementia, cardiovascular problems, gastrointestinal disease, liver disease, and weakening immune system[2]. Concerns over AUD remain more prevalent than ever as the pandemic's stay-at-home orders and relaxed alcohol restrictions heightened drinking patterns overall, markedly increasing the frequency of drinking past the recommended limit and binging[3]. Abstinence-based AUD treatments have limited success and often lead to cycles of consumption and relapse, but previous pre-clinical studies of medications to target excessive, uncontrollable alcohol consumption show more promising results[4]. Development of such interventions requires pre-clinical research to address dependence, a hallmark feature of AUDs. Dependence poses great challenges to controlling drinking behavior by increasing tolerance, which requires elevated drinking to attain previously pleasurable effects, and distressing withdrawal symptoms upon stopping alcohol intake[5].

In the brain, alcohol obstructs a delicate signaling balance at the synapse, resulting in disrupted cognitive, psychosocial, and regulatory functioning that vary by exposure. Alcohol is known as a depressant in acute use due to its initial ability to suppress excitatory and enhance inhibitory signaling, especially through the main inhibitory neurotransmitter gamma-aminobutyric acid (GABA) pathway. However, upon chronic exposure, the brain compensates for the repetitive homeostasis shift by changing concentration and activity of neurotransmitters and neuropeptides to amplify excitatory signaling. No longer does alcohol have significant withholding effects of excitatory neurotransmitters, and upon its withdrawal, there is a shift

towards a state of excessive excitation. Such is the case for glutamate-detecting α-amino-3-hydroxy-5-methyl-4-isoxazolepropionic acid receptor (AMPAR), which mediates a significant amount of excitatory signaling in the mammalian brain.

AMPARs are tetramer ion channels composed of various combinations of GluA1-4 subunits, each of which are coded by different genes and the unique composition of each AMPA receptor determines the function of the receptor. In general, upon binding to glutamate, the transmembrane pore of the AMPAR opens for Na^+ to flux into the neuron and increase the membrane potential. If the membrane depolarizes enough to exceed a threshold, an action potential is fired. This in turn triggers voltage-gated Ca^{2+} channels to open and activate Calmodulin, which then activates protein kinases such as Calcium/Calmodulin-Dependent Protein Kinase II (CaMKII). CaMKII can then upregulate excitatory signaling by phosphorylating AMPAR for increased Na^+ conductance, prolonging its anchoring onto the membrane and moving intracellular stores of AMPAR onto the membrane for higher density[6]. AMPARs are known to be remarkably dynamic, interacting with regulatory proteins that bind to specific subunits to affect receptor expression and activity accordingly. Therefore, the density and magnitude of AMPAR at the postsynaptic membrane is correlated to learning and memory; in pathological context such as addiction, drugs can hijack this pathway to highly appraise themselves and promote compulsive drug-seeking behavior[7]. Despite its ties to neuroplasticity and anxiety-like symptoms as observed in dependence, the exact role and mechanism as to which AMPAR has on the onset of dependence remains unknown. However, the GluA1 subunit is suspected to be particularly influential in alcohol reinforcement behavior given its role in modulating AMPAR trafficking and having higher activity upon alcohol intake in mice models[8].

While much is known about acute alcohol intake, reinforcement, and AMPAR, more recent data show that AMPAR activity is dysregulated in mice and rats with a history of dependence. A widely used and studied animal model that is also favorable to alcohol dependence research is the C57BL/6J strain mice. Unlike most mice, the C57BL/6J mice can quickly reduce taste aversion and show alcohol-seeking behavior. In addition, they age and develop numerous pathologies similar to those in humans, including immunological and cellular pathways upon chronic drinking[9]. Given the ability to closely replicate human conditions, utilizing this animal model will enable greater exploration of molecular targets without additional concerns that come with clinical research such as human genetic and lifestyle variability, experiment duration, attrition, and more stringent human research ethics. The mice model, upon undergoing well-established Chronic Intermittent Ethanol (CIE) Exposure, was shown to develop symptoms characteristic of alcohol dependence such as tolerance to aversive ethanol effects, persistent anxiety upon withdrawal, and elevated drinking behavior[10]. The method utilized intermittent exposure separated into cycles with breaks in between as opposed to continuous to clear out alcohol within subjects and repeatedly induce withdrawal syndrome. Within the mice's 24-hour endogenous circadian rhythm, it was found that 16-hour vapor exposure followed by 8-hour of fresh air induced most intense withdrawal periods[11]. Furthermore, intermittent exposure was shown to lessen taste aversion and increase tolerance in mice more than continuous exposure, elevating subsequent consumption[12]. Physiologically, CIE Exposure was also shown to increase basal glutamate levels in the Nucleus Accumbens[13], as well as upregulate AMPAR subunit concentrations and activity to induce plasticity-like state in the Amygdala and Insular Cortex upon 12 sessions of exposure[14].

The Amygdala (AMY), Prefrontal Cortex (PFC), Insular Cortex (INS), and Nucleus Accumbens (NAC) are brain regions particularly susceptible to excitatory signaling. Hence, they are speculated to be most impacted by glutamate pathway disruptions and sites where the onset of dependence occurs. Upon continued use, the Amygdala, known to regulate memory, stress, and emotions, will skew the reward pathway into favoring alcohol[15]. The Insular Cortex, responsible for interoception, will link the physiological responses denoting pleasure induced by alcohol into conscious urge[16]. The judgment and decision-making Prefrontal Cortex will compel action towards the impulse for the drug[17]. The Nucleus Accumbens would then remember the memories associated with the stimuli[18]. Intriguingly, the Amygdala, Prefrontal Cortex, and Insular Cortex are interconnected to the Nucleus Accumbens pathway[19]. This circuitry helps brain regions improve information collection and communication with one another to regulate the reward pathway (**Figure 1**).

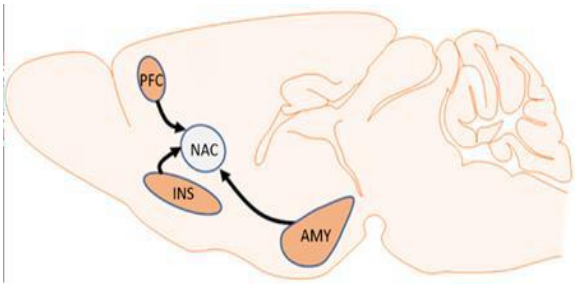

Figure 1. Interconnectedness of Brain Regions Susceptible to Excitatory Signaling. Connecting the Prefrontal Cortex (PFC), Insular Cortex (INS), and Amygdala (AMY) to the Nucleus Accumbens (NAC), improve information collection and communication with one another to regulate the reward pathway.

In addition to phosphorylated AMPAR subunits (such as pGluA1-Ser831), there is an interest in a category of auxiliary AMPAR proteins called TARPs (Transmembrane AMPA Receptor Regulatory Protein) that help anchor and provide a phosphorylation site (activated by CaMKII) to prolong the receptor's activity. TARPs are regionally selective, and TARP-γ8 especially has been measured in brain regions most susceptible to excitatory signaling and critical to conditioned drug use such as the Prefrontal Cortex, Insular Cortex, and Amygdala mentioned above. Yet, it is absent from the Nucleus Accumbens to which the other brain regions

project their axons (**Figure 2**). In a previous study conducted by the Hodge lab, The team found that knockout (+/-)mice, which has approximately 50% less TARP-γ8, showed same sensitivity and physiological response to alcohol to wild type but had reduced drinking frequency when alcohol was administered in lever-pressing (learned behavior)[20].

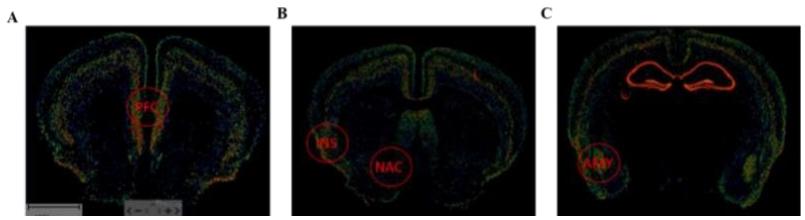

Figure 2. TARPy-8 Expression throughout Brain Regions within Reward Pathway. (**A**) Relative TARPy-8 expression at Prefrontal Cortex (PFC) locus. (**B**) Relative Insular Cortex (INS) and Nucleus Accumbens (NAC) loci, while INS has high TARPy-8 expression, NAC is devoid of it. (**C**) Relative TARPy-8 expression at Amygdala (AMY) locus.

This signifies that decreased TARP-γ8 expression correlates with reduced neural plasticity, though TARP-γ8's full role has yet to be extensively studied. Similarly, there are data suggesting Postsynaptic density protein 95 (PSD-95) mediates drinking behavior. PSD-95 knockouts, who lack the scaffolding protein that stabilizes AMPAR and other signaling and auxiliary proteins (such as TARP-γ8), showed decreased drinking than wildtype especially at higher ethanol concentrations[21]. **Figure 3** visualizes the location of GluA1, TARP-γ8, and PSD-95 at the synapse to demonstrate each component's roles in the glutamate pathway. Biochemical research quantifying the concentration and activity of proposed molecular components (GluA1,

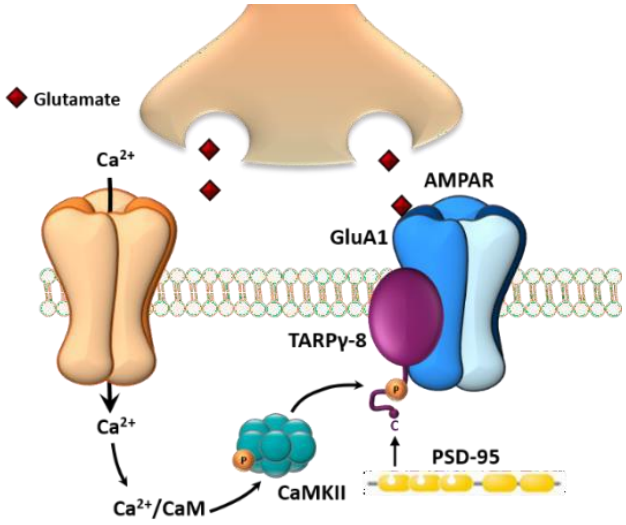

Figure 3. Glutamate Pathway Components at Postsynaptic Membrane. TARPγ-8 is an anchoring protein that additionally provides phosphorylation site to prolong activity of the AMPA Receptor. **GluA1**, an AMPA Receptor subunit, binds to glutamate and relays further excitatory signaling when activated. **PSD-95**, a scaffolding protein, stabilizes the AMPA Receptor and other signaling/auxiliary proteins such as TARPγ-8.

TARP-γ8, PSD-95 mRNA precursors and proteins) would verify the components' association to alcohol dependence as observed in previous studies.

The first objective of this study is to determine the efficacy of CIE exposure in inducing physiological response characteristic of alcohol dependence in the mouse model. After affirming sufficient exposure, gene expression of glutamatergic components suspected to be involved in the onset of dependence (GluA1, TARP-γ8, and PSD-95) will be quantified by brain region and condition. Lastly, since gene expression does not guarantee protein translation and activation, protein levels and phosphorylation will be compared to gene expression to observe whether changing protein concentration and activity contribute to establishing dependence.

METHODS

Chronic Intermittent Ethanol (CIE) Exposure

Subjects

Adult female C57BL/6J mice (n = 16 for Experiment 1, n = 17 for Experiment 2) from Jackson Laboratories (Bar Harbor, ME) arrived at the facility at the age of 12 weeks and were group-housed (4/cage in Experiment 1, 5/cage in Experiment 2) in polycarbonate cages (28 x 17 x 14 cm). Each cage was lined with corn cob bedding and contained a square mouse house and a cotton nestlet for environmental enrichment. Food (Purina Rodent Chow) and water were accessible ad libitum unless otherwise noted. Cages were housed in a vivarium maintained on a 12-hour light/dark cycle (lights on at 1900), with the temperature maintained at 21 ± 1 ºC and humidity of 40 ± 2%. Mice were given two weeks to adjust to the vivarium prior to the start of each experiment. All procedures done were in accordance with the NIH Guide to Care and Use of Laboratory Animals (National Research Council, 2011) and Institutional Animal Care and Use Committee (IACUC) at the University of North Carolina at Chapel Hill.

Vapor Chambers

A vapor chamber is an adjustable and efficient device used to expose cages to air vapor in a controlled manner. For these CIE experiments, we used vapor chambers purchased from La Jolla Alcohol Research, Inc.[22] to passively expose mice to alcohol by heating and vaporizing alcohol mixed with the ambient air and passing this alcohol-infused air into their home cages in 16-hour intervals (**Figure 4A**). Connecting the cages to a constant air flow through inlet (**a**) and outlet ports (**b**) created a closed system in which pressure was tightly maintained; the only air allowed in and out of the cages was vaporized ethanol. The air flow was pressurized so that there was rapid turnover of air in each cage throughout the 16-hour session. The set-up allowed for 8 cages to be concurrently connected. Half of the cages were connected to vaporized ethanol via tubing connected to a heated evaporation flask (**c**). Ethanol of 195 proof was loaded into a container connected to the flask (Glas-Col LLC, **d**), and its drip rate was adjusted by a pump for 2 mL/minute (**e**). Air flow (**f**) was adjusted to 16 mg/L for the duration of the experiment, as previous experimentation found that the flow rate provided vaporized EtOH for BAC levels to be within the target range of 180 - 240 mg/dL. The other half of the cages were only connected to the air flow to contain control group subjects. Both halves had the same air pressure.

Before each session, subjects were injected with pyrazole HCl (68 mg/kg), to inhibit ethanol metabolism and stabilize BAC throughout the session. The ethanol vapor mice were additionally injected with a priming dose of ethanol (1.6 g/kg: 8% (w/v) ethanol + pyrazole mixture). Injection volume was 20 mL/kg for all subjects. Subjects were loaded accordingly into flow-through cages (28 x 17 x 14 cm, as in group-housing), which were then placed into vapor chamber slots. Lights went on 2 hours into the session to maintain reverse light-dark cycle. Subjects were provided 4 pellets of food and a bottle of water for the duration of each session.

Cage positions within the apparatus were rotated throughout the week on respective sides (L side = ethanol vapor only; R side = Ambient Air only) to eliminate location in the chamber as a possible environmental variable for the experiment. Subjects underwent 16 hours of exposure per session for four consecutive sessions a cycle (Monday – Thursday nights). The project duration was 3 weeks, with 3 intermittent cycles of vapor (**Figure 4B**).

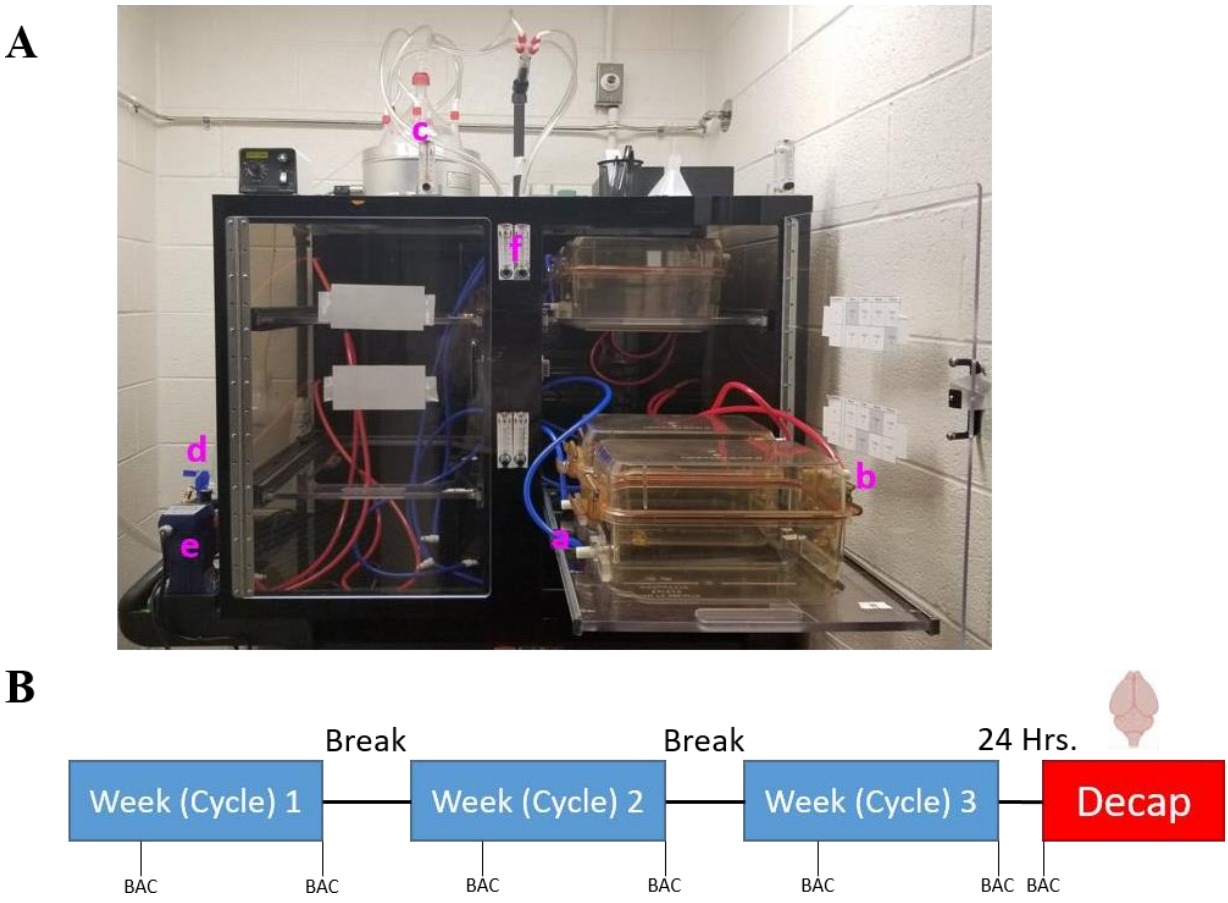

Figure 4. CIE Exposure via Vapor Chamber. (A) Vapor Chamber Setup. Constant air flow traveled through the cage from inlet (**a**) to outlet (**b**) ports and created an isolated, pressurized system. For subjects assigned to undergo CIE exposure, the inlet ports were coupled to the heated flask that vaporized ethanol (**c**). A container (**d**) filled with 195 proof ethanol replenished ethanol supply at a rate adjusted by a pump (**e**). A gauge (**f**) adjusted air flow rate to cycle through the system. **(B) Vapor Chamber Timeline** A cycle consisted of 4 consecutive days of 16-hour sessions. Cycles were separated by 3-day breaks. Each experiment underwent 3 cycles, and decapitation occurred 24 hours after completion of the last cycle.

Blood Alcohol Content (BAC)

Tail blood was collected immediately after the first and last CIE exposure session of each cycle (Tuesday and Friday morning). Blood was collected into Heparin-coated tubes to prevent coagulation. The tubes were centrifuged for 1 minute to separate and extract plasma. An AM1 Alcohol Analyzer (Analox Instruments, Lunenburg, MA, USA) measured BAC in mg/dL by measuring the rate of oxygen uptake by the alcohol to form acetaldehyde and hydrogen peroxide. Prior to use, the analox machine was calibrated with a 200 mg/dL alcohol standard. Then, 5 µL of plasma was injected into the machine for alcohol content to be measured (mg/dL). BAC verified whether subjects were exposed to sufficient and consistent levels of alcohol to establish dependence (180 – 240 mg/dL).

Tissue Extraction

After completing 3 cycles of vapor chamber exposure, mice were rapidly decapitated 24 hours after termination of the final overnight session. Whole-brain was quickly removed and flash-frozen in -40℃ Isopentane and individually stored in 15 mL conical tubes. Brains were stored at -80 ℃ until use. Tissue punches 1 mm thick from brain regions of interest [Prefrontal Cortex (PFC), Amygdala (AMY), Insular Cortex (INS), Nucleus Accumbens (NAC)] were (**Figure 5**) collected on a cryostat using a 1.0 mm diameter tissue dissection needle. Punches were bilateral for all regions except PFC, which was collected unilaterally. Tissue from isolated regions were placed in 2 mL mRNase-free plastic tubes for Experiment 1, 0.2 mL individual PCR tubes for Experiment 2. All tissue punches were stored at -80 ℃ until use. Additionally for Experiment 2 tissues, all tools, surfaces, containers had to be sterile or prepared with mRNase Decontamination Solution beforehand to prevent mRNase contamination.

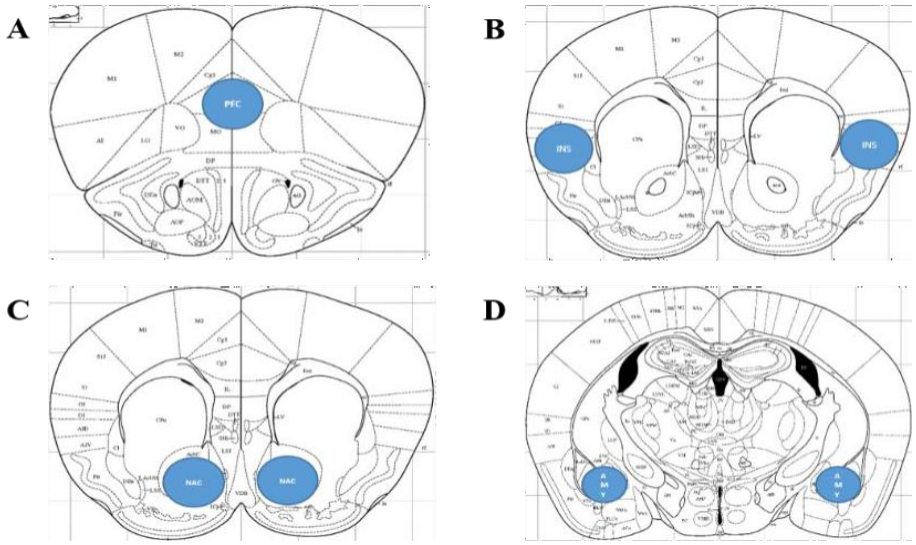

Figure 5. Approximate Locations of Brain Regions of Interest. The following regions were isolated (1 mm punches) from flash-frozen total brain in cryostat: **(A)** Prefrontal Cortex (PFC) **(B)** Insular Cortex (INS) **(C)** Nucleus Accumbens (NAC) **(D)** Amygdala (AMY).

Experiment 1: Quantifying Gene Expression

mRNA Extraction

Tissue punches were thawed, homogenized, and filtered to obtain samples of mRNA in accordance with instructions and solutions provided by RNeasy Micro Kit (QIAGEN). Tools and surfaces were sprayed with mRNAse Decontamination Solution prior to all experimentation and sterile nitrile gloves were used to prevent mRNase contamination.

In accordance with the RNeasy Micro Kit, β-Mercaptoethanol was added to the Buffer RLT Plus provided in the kit. β-Mercaptoethanol irreversibly denatured RNases by reducing disulfide bonds, rendering it harmless to mRNA in the sample. The Buffer RLT Plus homogenized and lysed cells to simplify separation in later steps. Genomic DNA contaminants were first filtered out by running buffer RLT Plus activated by 2-mercaptoethanol through gDNA Eliminator spin column and adding 70% ethanol to the supernatant to solubilize excess salts. Supernatant was then centrifuged with RNeasy MinElute spin column to trap mRNA inside

the filter. The filters were also centrifuged with Buffer RW1, RPE, and then 80% ethanol for further purification.

The column was then transferred over to a 1.5 mL collection tube, and 14 µL of mRNase-free water was pipetted onto the membrane. After incubating for 10 minutes at room temperature, the column was centrifuged to collect purified mRNA. NanoDrop 2000 Spectrophotometer (ThermoFisher Scientific, Waltham, MA) and the Nanodrop 2000/2000c software (Windows XP-SP2) analyzed the purity and concentration of extracted mRNA. Purity was indicated by the 260/280 ratio, with nearing 2.0 being favorable for pure mRNA samples. The absorbance value and nucleic acid concentration (ng/µL) directly indicated sample concentration.

One-Step Real-Time Quantitative Reverse Transcription Polymerase Chain Reaction (qRT-PCR)

Real-Time Quantitative Reverse Transcription PCR is a rapid, sensitive method to quantify nucleic acid sequences of interest. The experiment utilized fluorescent TaqMan RT-PCR probes with nucleic acid sequences complementary to that of the sequence of interest. When bound to the sequence, the fluorescent end of the probe is in proximity to the quencher end. The experiment also required thermally stable Taq Polymerases to perform reverse transcription, removing bound TaqMan probes along the way with exonuclease activity. Upon removal, the fluorescent end is disconnected from the quencher end, giving off a permanent signal. The fluorescent signal accumulates as more bound probes are freed by the amplification process. As opposed to the two-step process where single-stranded cDNA creation is separate from further amplification of cDNA into DNA, the one-step process was favored for its

efficiency, prevention of contamination, and easier processing of multiple samples for repetitive tests.

Prior to the amplification process, optimal sample concentration was found for each probe by creating a standard dilution curve. The pilot study found mRNA concentration of 0.8 ng/µL to be the lowest possible sample volume for detection given reaction condition constraints (2 hour total reaction time, 45 maximum cycles). All samples were diluted accordingly based on nucleic acid content found via the NanoDrop. Super mix was then prepared using kit materials as indicated in the QIAGEN OneStep RT-PCR Handbook, with respective target and GAPDH probes (TaqMan, see Appendix 1) to quantify mRNA amounts in brain regions of interest. GAPDH mRNA, which is ubiquitous in most cells and tissues, served as loading control to account for additional possible concentration discrepancies. Calculated amounts of super mix and samples were loaded onto respective wells in a 96-well plate and briefly centrifuged after sealing. Each sample was loaded in duplicates to minimize error and increase robustness of data.

After preparation, the plate was sealed and loaded onto Applied Biosystems Real-Time PCR StepOnePlus™, which changed temperatures sequentially for PCR reactions to occur. In the first step of qRT-PCR, reverse transcription occurred at 50°C for 30 minutes, creating cDNA using mRNA as the template strand at areas indicated by the target's primers. Following, the temperature was raised to 95°C in initial PCR activation for 15 minutes to inactivate the reverse transcriptase and denature cDNA strands off template mRNAs. Then, 3-step cycling followed PCR activation: denaturation (94°C) to take cDNA off mRNA templates, annealing (50-68°C) to attach fluorescent dNTPs between sites indicated by the primers, and extension (72°C) to create double-strand DNA from single-strand cDNA templates from the previous step.

Cycling steps repeated, with a minute for cooling between each, until enough target transcript was formed and fluorescence was visible against the background level. The average number of cycles until detection (C_T) was used to compare amounts of gene expression. Final extension (72°C) for 10 minutes allowed for any remaining elongation reactions to terminate. Applied Biosystems Real-Time PCR System Software (v.2.3) monitored and recorded the reaction processes, such as fold change and number of cycles.

Experiment 2: Quantifying Protein Expression Levels

Bicinchoninic Acid (BCA) Protein Assay

Bicinchoninic (BCA) Protein Assay quantified total protein of samples to ensure equal amounts of proteins were loaded per sample in later steps. Each sample was sonified in 120 µL of 1x Homogenization Buffer (5% SDS in 0.05M Tris, HALT Protease and Phosphatase Inhibitor Cocktail (EDTA Free) [100X]). As directed by the Pierce BCA Protein Assay Kit (ThermoFisher) User Guide, albumin standards were prepared, followed by a blue-green working reagent requiring 50:1 Reagent A (alkaline medium containing BCA) and Reagent B (containing Cu^{+2}), respectively. In a 96-well plate, 10 µL of albumin standards and each sample were loaded as duplicates, followed by 100 µL of working reagent. The plate was then incubated in 37°C water bath for 30 minutes and cooled to room temperature for 5 minutes. During that time, biuret reaction first occurred, where peptides containing three or more residues reduced Cu^{+2} to Cu^{+1}. A BCA-Cu complex then formed as two BCA molecules chelated to the Cu^{+1} ion, turning the solution purple. A spectrophotometer (SpectraMax 384Plus) then measured absorbance of each wells at 562 nm that directly correlates to protein concentration. A standard curve relating known albumin concentrations (µg/mL) and average absorbance values was then

formulated to estimate protein concentrations from absorbance values of sample wells. Duplicates were then averaged and expressed as units of µg/µL.

Gel Electrophoresis

When used in conjunction to ionic detergent SDS, gel electrophoresis separates sample content based on molecular size as proteins are denatured and uniformly negatively charged. In preparation for SDS-PAGE, blots were designed for each lane to contain respective protein concentrations, 6.25 µL of x4 Standard Buffer, 2.5 µL of x10 Reducing Agent, and diluted with sterilized water to 25 µL in volume. Sample volumes varied amongst brain regions and targets due to volume constraints and signaling clarity. AMY, INS, and NAC blots were loaded with 10 µg for blots designated to observe pGluA1-Ser831, TARPγ-8, and PSD-95, while PFC had 7.5 µg. Designated PSD-95 blots consistently used 5 µg across brain regions. Vortexed lane samples were heated in a 70°C water bath for 5 minutes, cooled in room temperature for 3 minutes, and centrifuged. Each 8% Polyacrylamide gel also had one lane with 12 µL of SeeBlue Plus2 Pre-stained ladder (ThermoFisher) to facilitate band identification. After running in 1x Tris-Buffered Saline, 0.1% Tween 20 Detergent (Sigma Aldrich), the contents of the gel were transferred onto a polyvinylidene fluoride (PVDF) membrane compatible with the iBlot2 Gel Transfer Device (ThermoFisher) via a semi-dry rapid transfer approach. The membrane was then stored in 1x Phosphate-Buffered Saline (PBS) until further use.

Immunoblot

Prior to each antibody exposure, membranes were gently rocked in 3% NGS blocking buffer (3% Normal Goat Serum (NGS) in 1M Tris Base pH 7.2, 5M NaCl, Tween20) for an hour. The blots were then incubated in 1:10,000 dilution of GAPDH primary antibody (Advanced ImmunoChemistry Inc.) in 3% NGS blocking buffer. After washing the blots with 1x

Phosphate-Buffered Saline with Tween 20 (PBST), followed by 1x Phosphate-Buffered Saline (PBS) alone, the blots were incubated in 1:10,000 dilution of Goat anti-Mouse secondary antibody (Jackson Laboratories) in 3% NGS blocking buffer. Blots were then rocked in ECL Select (Amersham) and imaged with ImageQuant LAS 4000 software (GE Healthcare) for chemiluminescent immunoreaction detection.

Following GAPDH detection, blots were washed in 1% NGS blocking buffer and incubated in target primary antibody for approximately 18 hours overnight in 4 °C. Primary antibodies were diluted as according to Appendix 2. After incubation, the blots were washed with 1x PBST and PBS. They were then incubated for 1 hour in 1:10,000 dilution of Goat anti-Rabbit secondary antibody (Jackson Laboratories) in 1% NGS blocking buffer. TARPγ-8 and pGluA1-Ser831 were then exposed to ECL Prime (Amersham), while PSD-95 was exposed to ECL Select (Amersham) for chemiluminescent immunoreaction detection in imaging.

Statistical Analysis

All statistical analyses were performed using Prism v.8.0 (GraphPad, La Jolla, CA). Relationship between body weight (g) and BAC (mg/dL) for each alcohol-exposed subject was analyzed per cycle using simple linear regression. In Experiment 2, fold change of alcohol-exposed and non-exposed subjects were compared using one-way unpaired t-test. Fold change represents the amount of gene expression amplified per cycle, and is found by the formula: $2^{-[(CT_{target}-C_{T_{GAPDH}}\,EtOH/air)-(C_{T_{target}}-C_{T_{GAPDH}}\,in\,air)]}$. Following, Experiment 3 compared the difference in target protein concentration between conditions. Target and GAPDH signals per sample measured by ImageQuant TL were expressed as target-to-GAPDH ratios. Each ratio of ethanol-exposed mice was compared to the average ratio for unexposed mice, then converted into percentages. In both Experiment 2 and 3 analyses, Grubbs test for outliers was performed

for both target and GAPDH measures per group. All figures were also made using Prism v.8.0, representing the means ± standard error of the means (SEM). For all statistical tests, alpha was set to 0.05.

RESULTS

The Vapor Chamber was a Consistent Method of CIE Exposure

A 2-way ANOVA revealed the effect of time ($F(2, 30) = 287.1$, $p < 0.0001$) in increasing BAC. Though experiment group alone ($F(1, 15) = 2.025$, $p = 0.1752$) did not show significant difference, experiment group coupled with time ($F(2, 30) = 7.428$, $p = 0.0024$) showed considerable discrepancies in BAC values. The trends indicate that the CIE exposure method induced consistent results across different experiments, in which BAC varied considerably by time points. Post-hoc determined significance from time resulting from Cycle 1. In both experiments, BACs were intentionally lowered in Week 1 to help subjects acclimate to the protocol as tolerance was expected over time. Flow rates varied accordingly to obtain optimal BAC range, and this proved successful in maintaining stable BAC levels across weeks.

In both experiments, target BAC levels of 180-240 mg/dL were met in only the last two cycles of the three-cycle process. The weekly mean BAC levels were 105.26 (Week 1), 211.88 (Week 2), and 212.90 mg/dL (Week 3) for Experiment 1 and 94.98 (Week 1), 229.32 (Week 2), and 249.12 mg/dL (Week 3) for Experiment 2. Linear regressions for each cycle between weight (g) and BAC (mg/dL) found weak to no correlation between the two factors (**Figure 6**). R^2 values were found to measure the proportion of BAC variance from the line-of-best-fit explained by weight. Experiment 2 subjects had R^2 values of 0.2449 (Cycle 1), 0.4355 (Cycle 2), 0.2493 (Cycle 3) while Experiment 3 subjects had R^2 values of 0.0416 (Cycle 1), 0.0067 (Cycle 2), 0.2098 (Cycle 3). Correlation coefficient (R), which more directly quantifies the association

between weight and BAC, was +0.4949 (Cycle 1), -0.6599 (Cycle 2), and +0.4993 (Cycle 3) for Experiment 2 subjects and -0.2040 (Cycle 1), -0.0819 (Cycle 2), and +0.4580 (Cycle 3) for Experiment 3 subjects. The magnitude of most correlation coefficients was of moderate strength, but fluctuating direction indicates that weight was not a confounding variable to the amount of alcohol exposure.

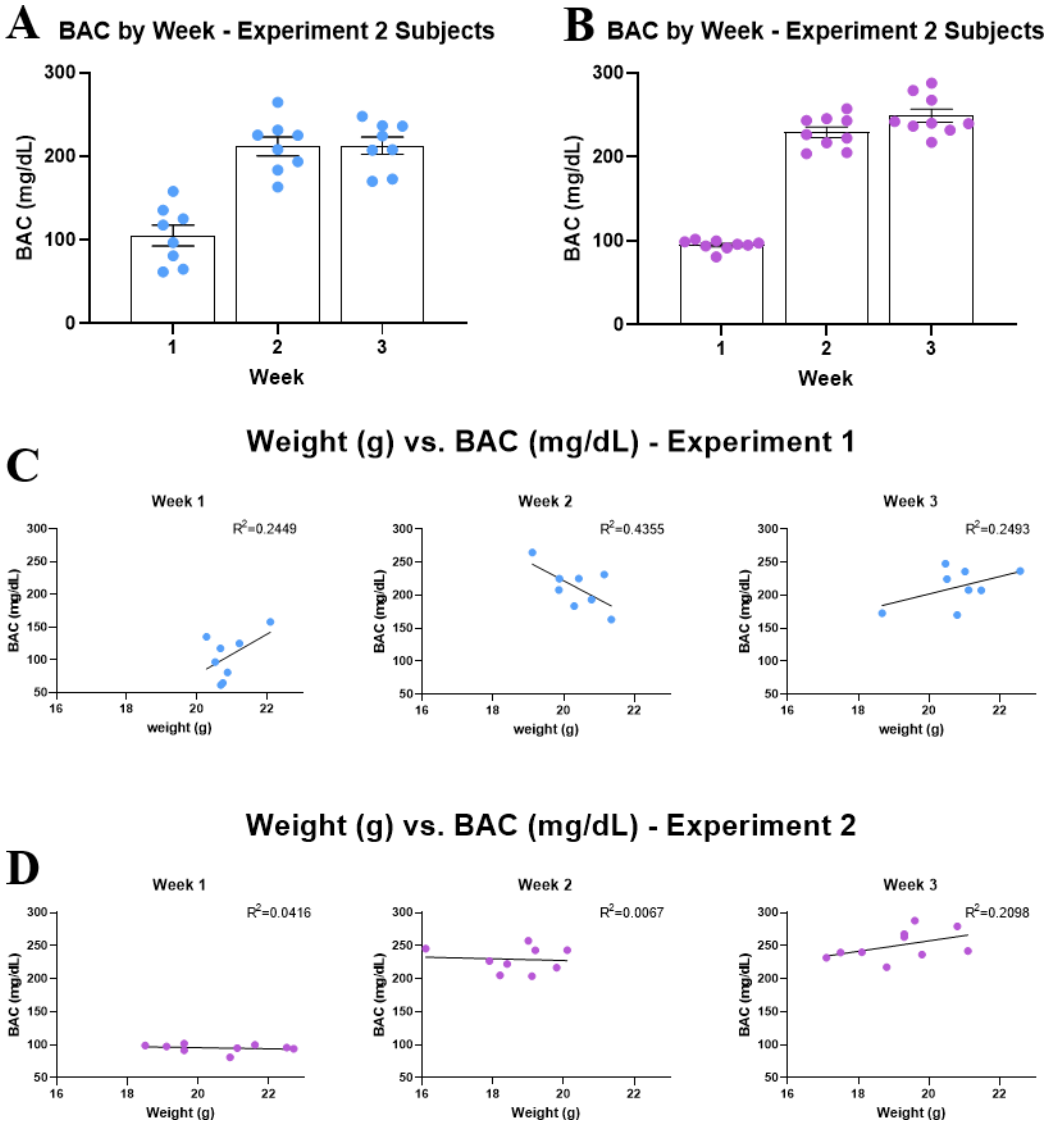

Figure 6. Measurement Vapor Chamber Efficacy in CIE Exposure. Figures analyze weekly measures of BAC for subjects within Experiment 1 and 2. (**A**) Comparison of Weekly BACs for subjects in Experiment 1. (**B**) Comparison of Weekly BACs for subjects in Experiment 2. (**C**) Linear regression line relating weights of subjects in Experiment 1 weighed weekly (g) vs. BAC (mg/dL). (**D**) Linear regression line relating weights of subjects in Experiment 2 weighed weekly (g) vs. BAC (mg/dL).

Experiment 1: Gene Expression Changes of Glutamatergic Components Varied Across Brain Regions

RNA Extraction

RNA Extraction data are reported for qRT-PCR. The 260/280 ratio is a comparison of a substance's absorbance value at 260 and 280 nm. Since different compounds have specific absorption affinities at respective wavelengths, the ratio determines the purity of a sample; pure mRNA has a 260/280 ratio of 2.0. The ratios were consistently around 2.0 for all brain regions within both experiment groups (**Figure 7B**), assuring that all samples contained pure, extracted mRNA without any DNA or protein to confound the results.

Absorbance values directly correlate to nucleic acid concentration (ng/μL), as more concentrated samples would absorb more light and decrease residual transmittance read by the machine. Measuring absorbance enabled relative comparisons of mRNA concentration between brain regions, as well as ensure equal concentrations of mRNA are analyzed in qRT-PCR. The Amygdala, Insular Cortex, and Nucleus Accumbens showed high concentration of RNA with consistent levels between each subject (low inter-subject variability). The Prefrontal Cortex had consistent levels as well but was less concentrated, as expected, given it was only a unilateral punch.

qRT-PCR

Fold change reported from qRT-PCR compared relative target gene expression levels to control gene (GAPDH) in each brain region. More specifically, it represents the average amount

of gene expression amplified using the sample's mRNA as templates per cycle in the gene amplification stage of PCR (**Figure 7A**).

A

	PFC	NAC	INS	AMYG
GRIA1	-	-	↑	↑
CACNG8	↓	-	-	↑
DLG4	-	-	↑	↑

B

PFC		NAC		INS		AMY	
Mean	SEM	Mean	SEM	Mean	SEM	Mean	SEM
2.000	0.021	2.028	0.016	1.989	0.011	2.051	0.012

Figure 7. Summary of Experiment 1. (**A**) Results from qRT-PCR quantifying difference in gene expression between Air (Control) and CIE Exposed mice are compiled by probe for brain regions of interest. (**B**) RNA extraction was performed in 4 rounds based on brain region. Each extraction's mean 260/280 ratio quantified the success in purification, while SEM measured precision between samples.

GRIA1

GRIA1 is the gene that encodes the GluA1 subunit of the AMPA receptor. As shown in **Figure 8**, GRIA1 was significantly upregulated in the Amygdala (t (13) = 2.063, p = 0.030) and Insular Cortex (t (13) = 2.329, p = 0.037). There were also slight trends of downregulation in Prefrontal Cortex (t (12) = 0.981, p = 0.173) and almost no change in Nucleus Accumbens (t (14) = 0.675, p = 0.510).

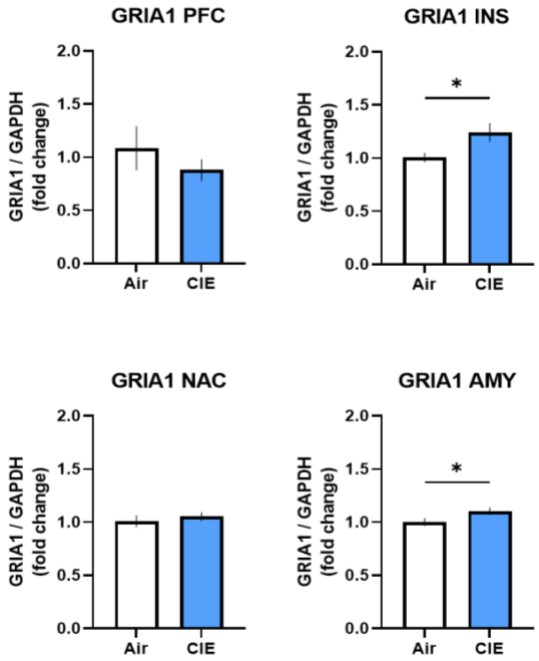

Figure 8. qRT-PCR quantifying GRIA1 mRNA. Figures compare average fold change in by brain region per cycle between Air (control) and CIE Exposed subjects in Experiment 1. (**A**) GRIA1 Fold Change in Air vs. CIE Exposed in Prefrontal Cortex. (**B**) GRIA1 Fold Change in Air vs. CIE Exposed in Insular Cortex. (**C**) GRIA1 Fold Change in Air vs. CIE Exposed in Nucleus Accumbens. (**D**) GRIA1 Fold Change in Air vs. CIE Exposed in Amygdala.

CACNG8

CACNG8, precursor for phosphorylation site and anchoring protein TARP-γ8, was significantly upregulated in only the Amygdala (t (12) = 2.375, p = 0.018), but strikingly significantly downregulated in the Prefrontal Cortex (t (13) = 2.415, p = 0.016). The Insular Cortex (t (13) = 0.257, p = 0.801) and Nucleus Accumbens (t (13) = 1.790, p = 0.097) had slight upregulation but were closer to observing no change (**Figure 9**).

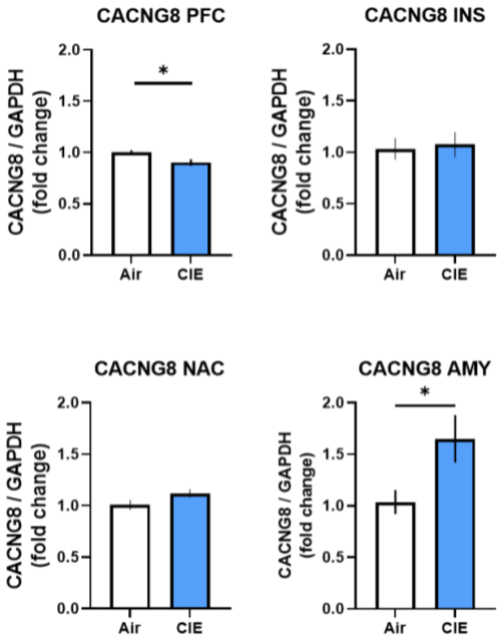

Figure 9. qRT-PCR quantifying CACNG8 mRNA. Figures compare average fold change in by brain region per cycle between Air (control) and CIE Exposed subjects in Experiment 1. (**A**) CACNG8 Fold Change in Air vs. CIE Exposed in Prefrontal Cortex. (**B**) CACNG8 Fold Change in Air vs. CIE Exposed in Insular Cortex. (**C**) CACNG8 Fold Change in Air vs. CIE Exposed in Nucleus Accumbens. (**D**) CACNG8 Fold Change in Air vs. CIE Exposed in Amygdala.

DLG4

Precursor for scaffolding protein PSD-95, DLG4, was significantly upregulated in the Insular Cortex (t (11) = 2.258, p = 0.023) and Amygdala (t (13) = 2.077, p = 0.029) and had

trends of upregulation in the Prefrontal Cortex (t (11) = 1.130, p = 0.141) and Nucleus Accumbens (t (14) = 1.051, p = 0.155) (**Figure 10**).

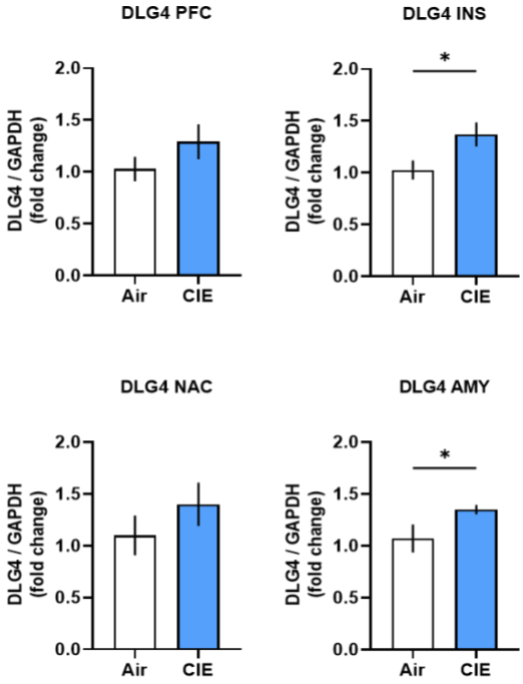

Figure 10. qRT-PCR quantifying DLG4 mRNA. Figures compare average fold change in by brain region per cycle between Air (control) and CIE Exposed subjects in Experiment 1. (**A**) DLG4 Fold Change in Air vs. CIE Exposed in Prefrontal Cortex. (**B**) DLG4 Fold Change in Air vs. CIE Exposed in Insular Cortex. (**C**) DLG4 Fold Change in Air vs. CIE Exposed in Nucleus Accumbens. (**D**) DLG4 Fold Change in Air vs. CIE Exposed in Amygdala.

Experiment 2: Protein Translation Loosely Followed Gene Expression

By measuring relative protein concentration, the experiment determined whether observed gene expression changes subsequently altered protein concentrations to affect glutamate pathway functioning. The optical densities from chemiluminescent immunoreaction detection of protein targets were plotted in comparison to parts of the air control group (**Figure 11**).

	PFC	NAC	INS	AMYG
pGluA1	-	↑	↑	-
TARPy-8	-	-	-	-
PSD-95	-	-	-	-

Figure 11. Summary of Experiment 2. Results from western blots quantifying difference in protein amount between Air (control) and CIE Exposed mice are compiled by target for brain regions of interest.

pGluA1-Ser831

Upon probing for active GluA1 phosphorylated at Ser831, significant upregulation was found for the Insular Cortex ($t(12) = 2.233$, $p = 0.023$) and Nucleus Accumbens ($t(13) = 2.569$, $p = 0.012$). While not significant, the Amygdala ($t(14) = 1.312$, $p = 0.105$) and Prefrontal Cortex ($t(14) = 1.650$, $p = 0.061$) had trends of upregulation (**Figure 12**).

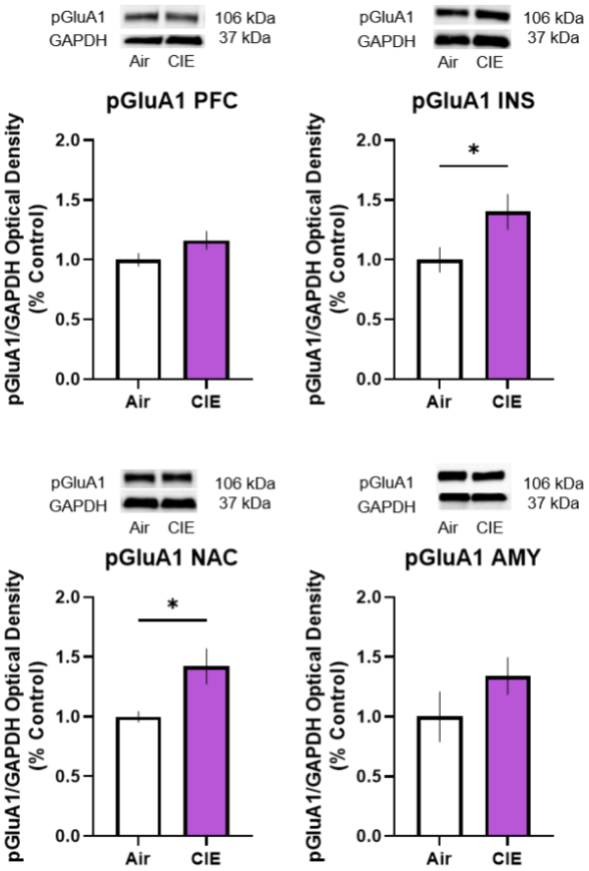

Figure 12. Optical Density quantifying Relative pGluA1-Ser831. Figures observe relative protein concentration of experimental groups in comparison to Air (control) mice by brain region in Experiment 2. (**A**) Relative pGluA1-Ser831 in Air vs. CIE Exposed in Prefrontal Cortex (**B**) Relative pGluA1-Ser831 in Air vs. CIE Exposed in Insular Cortex (**C**) Relative pGluA1-Ser831 in Air vs. CIE Exposed in Nucleus Accumbens. (**D**) Relative pGluA1-Ser831 in Air vs. CIE Exposed in Amygdala.

TARPγ-8

TARP-γ8 did not show any significant changes, but trends of upregulation with varying degrees in all regions: Prefrontal Cortex (t (14) = 1.337, 0.101), Insular Cortex (t (13) = 1.494, p = 0.080), Nucleus Accumbens (t (11) = 0.318, p = 0.378), Amygdala (t (15) = 0.203, p = 0.421) (**Figure 13**).

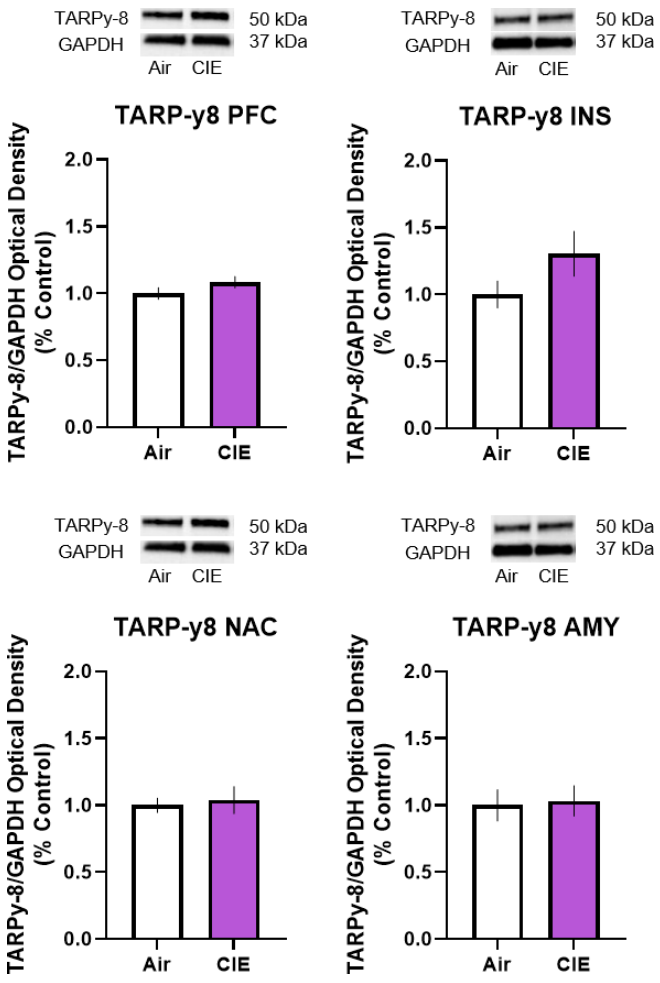

Figure 13. Optical Density quantifying Relative TARPy-8. Figures observe relative protein concentration of experimental groups in comparison to Air (control) mice by brain region in Experiment 2. (**A**) Relative TARPy-8 in Air vs. CIE Exposed in Prefrontal Cortex. (**B**) Relative TARPy-8 in Air vs. CIE Exposed in Insular Cortex. (**C**) Relative TARPy-8 in Air vs. CIE Exposed in Nucleus Accumbens. (**D**) Relative TARPy-8 in Air vs. CIE Exposed in Amygdala.

PSD-95

PSD-95 also did not show any significant changes and was closer to showing no change (**Figure 14**). However, there was duality in directionality, as Amygdala (t (14) = 0.137, p = 0.446) and Prefrontal Cortex (t (13) = 0.692, p = 0.251) showed slight upregulation while Insular Cortex (t (14) = 0.057, p = 0.478) and Nucleus Accumbens (t (14) = 0.959, p = 0.177) had slight downregulation.

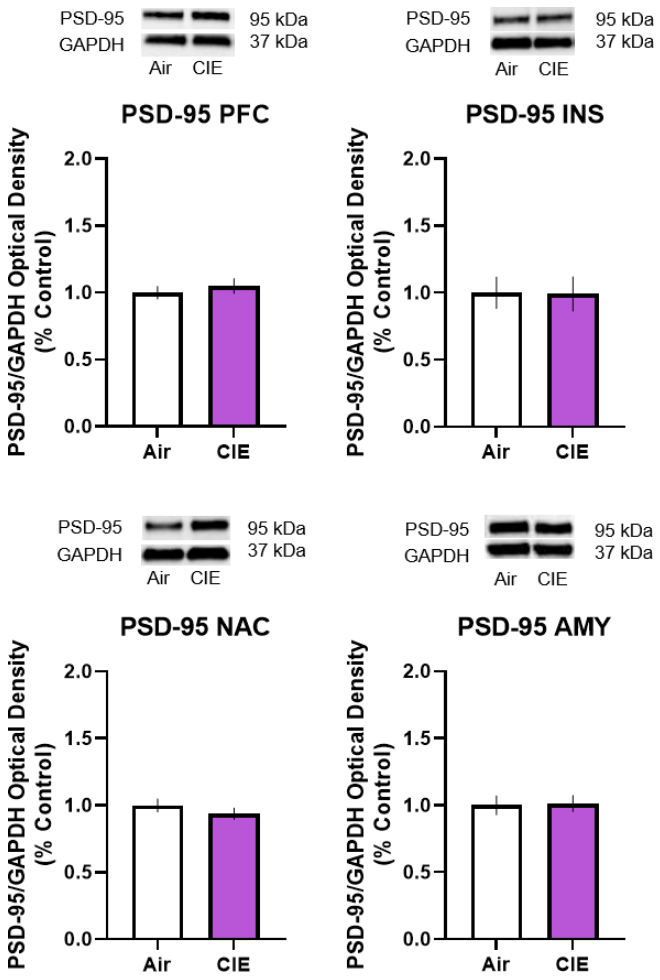

Figure 14. Optical Density quantifying Relative PSD-95. Figures observe relative protein concentration of experimental groups in comparison to Air (control) mice by brain region in Experiment 2. (**A**) Relative PSD-95 in Air vs. CIE Exposed in Prefrontal Cortex. (**B**) Relative PSD-95 in Air vs. CIE Exposed in Insular Cortex. (**C**) Relative PSD-95 in Air vs. CIE Exposed in Nucleus Accumbens. (**D**) Relative PSD-95 in Air vs. CIE Exposed in Amygdala.

DISCUSSION

The purpose of the study was to observe molecular components within the glutamatergic pathway affected by dependence-inducing alcohol levels. Identifying directionality and significant changes amongst components within the pathway would have specified possible pharmacological targets for further study into possible drug development for lessening alcohol dependence. In inducing alcohol dependence by CIE Exposure, the vapor chamber proved to be a consistent method to induce similar BAC levels at same timepoints between subjects of Experiment 1 and 2.

The goal of Experiment 1 was to measure levels of gene expression of targets hypothesized to be critical for regulating alcohol drinking and dependence. Indeed, it was found that amongst the three gene targets GRIA1 (GluA1 precursor), CACNG8 (TARPγ-8 precursor), and DLG4 (PSD-95 precursor), significant gene expression changes occurred specific to brain region. Particularly, the Amygdala upregulated expression in all three targets, and the Insular Cortex similarly followed the trend. However, the Prefrontal Cortex opposed the trend significantly in CACNG8 and somewhat in GRIA1, while the Nucleus Accumbens showed no effect. The downregulated changes observed from the Prefrontal Cortex opposing patterns in the Amygdala and Insular Cortex are speculated to be combinatory in effect to the common region. In this instance, the brain regions seemed to negate one another, perhaps to maintain neural homeostasis.

Experiment 1 observations were consistent with previous data showing how each brain region modulates its specific glutamatergic effect onto the Nucleus Accumbens to influence the reward pathway. Though more research about the Insular Cortex is currently underway, the Amygdala's heightened glutamatergic gene expression is supported by significant increase in

operant self-administration of sweetened alcohol-drinking mice than their sucrose-drinking control counterparts. Closer observations showed the Nucleus Accumbens-projecting neurons of alcohol-drinking mice to have higher excitatory postsynaptic activity from elevated GluA1 phosphorylation and concentration. The findings were further ensured by blunted alcohol self-administration upon inhibited excitatory current and GluA1 trafficking and activity[24]. Conversely, the Prefrontal Cortex is known to regulate cognitive control and impulse inhibition, counteracting the upregulating brain regions via top-down regulation. Inhibiting CAMKII activity in the Prefrontal Cortex (a phosphorylation step to prolong AMPAR at the membrane, Figure 1) was shown to reduce inhibition against reinforcing effects of alcohol, escalating drinking patterns[25].

Based on the complexity of the reward pathway, other regions in this circuitry may contribute to the onset of dependence. An additional area that projects onto the Nucleus Accumbens is the Hippocampus, which has a major role in learning and memory. Similar to the Amygdala's, glutamatergic projections from the Hippocampus has shown to induce craving-associated behaviors upon associations built from previously neutral cues[26]. While not reported in this study, the Hodge lab continues to widen the examination to include other regions for a more comprehensive understanding of the neurological impact of prolonged alcohol use.

When respective protein concentrations were measured in Experiment 2, it was shown that concentration levels did not follow the pattern for gene expression. Even with miniscule protein concentration changes in TARPγ-8, the downregulation of mRNA synthesis that brought interest to the Prefrontal Cortex was contradicted by the protein's slight upregulation. PSD-95 was also almost identical to control but differed in its slight directionality in the Prefrontal Cortex, Insular Cortex, and Nucleus Accumbens. pGluA1-Ser831 most closely reflected

directionality of gene expression, with significance also in the Insular Cortex. However, pGluA1-Ser831 was also shown to be significantly upregulated in the Nucleus Accumbens, inconsistent with the lack of significant change from Experiment 2. Because pGluA1-Ser831 is also the phosphorylated (active) form of the protein, it introduces possible confounding mechanisms than that involved with GluA1's gene expression. Observing the more direct effect of gene expression changes in GRIA1 would require quantification of tGluA1 (includes both not phosphorylated and phosphorylated GluA1 subunit).

Inconsistency between the study's patterns of gene expression and protein translation may raise questions about its validity. However, this issue is common within the many fields involving the association between mRNA and protein synthesis. The relationship between mRNA and protein levels is more dynamic and complex than the smooth proceeding from gene to mRNA (transcription) to protein peptide sequence (translation) that the central dogma seems to suggest. Rather, protein translation from mRNA alone requires additional considerations such as the duration of transcription itself, modifications to sequence and higher structure, lull in between processes, transportation of the protein to its respective location, and possible mRNA and peptide degradation. Therefore, comparison between protein and mRNA concentration requires more consideration as to how components may interact with its cellular environment[23].

Significant trends in gene expression and protein synthesis despite lower ethanol exposure levels than targeted, as well as explanations for the discrepancy in gene expression and protein translation patterns, provide possibilities for more comprehensive and coherent results. A possible modification for Experiment 1 would be to account for subjects' differing physiological responses at different timepoints of CIE exposure. More specifically, finding ways to safely increase BAC levels throughout Cycle 1, such as fine-tuning ethanol and metabolism-blocking

pyrazole levels, would ensure that subjects are receiving sufficient exposure more like that of the literature. As for Experiment 2, future experiments observing gene expression changes of more brain regions also linked to the Nucleus Accumbens may broaden understanding of the regulation involved within the pathway to maintain its delicate balance. In Experiment 3, quantifying the more directly encompassing tGluA1 could ensure that truly protein levels are affected by the gene expression changes, as well as provide insight into how phosphorylation activity might be regulated. Most importantly, future experiments varying the time of subjects' decapitation (more likely deferring) may allow for protein amounts to more closely resemble alterations seen in gene expression. Replicating the study with modifications specified for each experiment is recommended to substantiate the cellular mechanism of alcohol dependence for future development of treatments.

CONCLUSION

The results of this study show that in brain regions that regulate the reward pathway, there are region-specific differences in gene expression changes of AMPAR-related molecular targets (GluA1, TARPγ-8, and PSD-95) hypothesized to impact the onset of alcohol dependence. In particular, the observed brain regions seem to project mediating effects onto the Nucleus Accumbens in an attempt to maintain neural homeostasis. Upon comparing relative protein concentrations of corresponding genes in the same regions, significant changes did not directly reflect those observed in measuring gene expressions. In consideration of additional time and cellular environmental factors required for gene transcription to be followed by protein translation, future experiments may observe difference in protein concentrations upon varied decapitation times, as well as compare between total and phosphorylated protein targets.

Identifying changes upon chronic alcohol exposure may specify pharmacological targets and improve efficacy for addiction interventions.

REFERENCES

(1) Alcohol Facts and Statistics | National Institute on Alcohol Abuse and Alcoholism (NIAAA) https://www.niaaa.nih.gov/publications/brochures-and-fact-sheets/alcohol-facts-and-statistics.

(2) Understanding Alcohol Abuse & Medical Issues https://www.alcohol.org/comorbid/.

(3) News, T. H. M.; Affairs, P. Study Holds Warning on Pandemic Drinking. *Harvard Gazette*, 2022.

(4) Interventions and Assessments | Alcohol, Other Drugs, and Health: Current Evidence https://www.bu.edu/aodhealth/tag/interventions-and-assessments/.

(5) Becker, H. C. Alcohol Dependence, Withdrawal, and Relapse. *Alcohol Res Health* **2008**, *31* (4), 348–361.

(6) Chater, T. E.; Goda, Y. The Role of AMPA Receptors in Postsynaptic Mechanisms of Synaptic Plasticity. *Frontiers in Cellular Neuroscience* **2014**, *8*.

(7) Agoglia, A. E.; Holstein, S. E.; Reid, G.; Hodge, C. W. CaMKIIα-GluA1 Activity Underlies Vulnerability to Adolescent Binge Alcohol Drinking. *Alcohol Clin Exp Res* **2015**, *39* (9), 1680–1690. https://doi.org/10.1111/acer.12819.

(8) Rhodes, J. S.; Best, K.; Belknap, J. K.; Finn, D. A.; Crabbe, J. C. Evaluation of a Simple Model of Ethanol Drinking to Intoxication in C57BL/6J Mice. *Physiol Behav* **2005**, *84* (1), 53–63. https://doi.org/10.1016/j.physbeh.2004.10.007.

(9) Lopez, M. F.; Griffin, W. C.; Melendez, R. I.; Becker, H. C. Repeated Cycles of Chronic Intermittent Ethanol Exposure Leads to the Development of Tolerance to Aversive Effects of Ethanol in C57BL/6J Mice. *Alcohol Clin Exp Res* **2012**, *36* (7), 1180–1187. https://doi.org/10.1111/j.1530-0277.2011.01717.x.

(10) Goldstein, D. B. Relationship of Alcohol Dose to Intensity of Withdrawal Signs in Mice. *J Pharmacol Exp Ther* **1972**, *180* (2), 203–215.

(11) O'Dell, L. E.; Roberts, A. J.; Smith, R. T.; Koob, G. F. Enhanced Alcohol Self-Administration after Intermittent versus Continuous Alcohol Vapor Exposure. *Alcohol Clin Exp Res* **2004**, *28* (11), 1676–1682. https://doi.org/10.1097/01.alc.0000145781.11923.4e.

(12) Griffin, W. C.; Ramachandra, V. S.; Knackstedt, L. A.; Becker, H. C. Repeated Cycles of Chronic Intermittent Ethanol Exposure Increases Basal Glutamate in the Nucleus Accumbens of Mice without Affecting Glutamate Transport. *Frontiers in Pharmacology* **2015**, *6*.

(13) McGinnis, M. M.; Parrish, B. C.; McCool, B. A. Withdrawal from Chronic Ethanol Exposure Increases Postsynaptic Glutamate Function of Insular Cortex Projections to the Rat Basolateral Amygdala. *Neuropharmacology* **2020**, *172*, 108129. https://doi.org/10.1016/j.neuropharm.2020.108129.

(14) Gilpin, N. W.; Herman, M. A.; Roberto, M. The Central Amygdala as an Integrative Hub for Anxiety and Alcohol Use Disorders. *Biological Psychiatry* **2015**, *77* (10), 859–869. https://doi.org/10.1016/j.biopsych.2014.09.008.

(15) Campbell, E. J.; Lawrence, A. J. It's More than Just Interoception: The Insular Cortex Involvement in Alcohol Use Disorder. *J Neurochem* **2021**, *157* (5), 1644–1651. https://doi.org/10.1111/jnc.15310.

(16) Encoding of the Intent to Drink Alcohol by the Prefrontal Cortex Is Blunted in Rats with a Family History of Excessive Drinking | eNeuro https://www.eneuro.org/content/6/4/ENEURO.0489-18.2019 (accessed 2022 -04 -01).

(17) The Role of Nucleus Accumbens in Addiction | UK Rehab https://www.uk-rehab.com/addiction/psychology/nucleus-accumbens/ (accessed 2022 -04 -01).

(18) Mesolimbic Pathway - an overview | ScienceDirect Topics https://www.sciencedirect.com/topics/neuroscience/mesolimbic-pathway (accessed 2022 -04 -01).

(19) Faccidomo, S. A Novel Glutamatergic Mechanism for the Treatment of Cocaine and Opioid Use Disorders, and Co-Occurring Anxiety.

(20) Park, J.; Chavez, A. E.; Mineur, Y. S.; Morimoto-Tomita, M.; Lutzu, S.; Kim, K. S.; Picciotto, M. R.; Castillo, P. E.; Tomita, S. CaMKII Phosphorylation of TARPγ-8 Is a Mediator of LTP and Learning and Memory. *Neuron* **2016**, *92* (1), 75–83. https://doi.org/10.1016/j.neuron.2016.09.002.

(21) Camp, M. C.; Feyder, M.; Ihne, J.; Palachick, B.; Hurd, B.; Karlsson, R.-M.; Noronha, B.; Chen, Y.-C.; Coba, M. P.; Grant, S. G. N.; Holmes, A. A Novel Role for PSD-95 in Mediating Ethanol Intoxication, Drinking and Place Preference. *Addict Biol* **2011**, *16* (3), 428–439. https://doi.org/10.1111/j.1369-1600.2010.00282.x.

(22) Kimbrough, A. Intermittent Access to Ethanol Drinking facilitates the Transition to Excessive Drinking after Chronic Ethanol Vapor Exposure. *LJARI* **2017**, *41* (8), 1502–1509. https://doi.org/10.1111/acer.13434.

(23) Liu, Y.; Beyer, A.; Aebersold, R. On the Dependency of Cellular Protein Levels on MRNA Abundance. *Cell* **2016**, *165* (3), 535–550. https://doi.org/10.1016/j.cell.2016.03.014.

(24) Faccidomo, S.; Cogan, E. S.; Hon, O. J.; Hoffman, J. L.; Saunders, B. L.; Eastman, V. R.; Kim, M.; Taylor, S. M.; McElligott, Z. A.; Hodge, C. W. Calcium-Permeable AMPA Receptor Activity and GluA1 Trafficking in the Basolateral Amygdala Regulate Operant Alcohol Self-Administration. *Addict Biol* **2021**, *26* (5), e13049. https://doi.org/10.1111/adb.13049.

(25) Faccidomo, S.; Reid, G. T.; Agoglia, A. E.; Ademola, S. A.; Hodge, C. W. CaMKII Inhibition in the Prefrontal Cortex Specifically Increases the Positive Reinforcing Effects of Sweetened Alcohol in C57BL/6J Mice. *Behav Brain Res* **2016**, *298* (Pt B), 286–290. https://doi.org/10.1016/j.bbr.2015.11.018.

(26) Alasmari, F.; Goodwani, S.; McCullumsmith, R. E.; Sari, Y. Role of Glutamatergic System and Mesocorticolimbic Circuits in Alcohol Dependence. *Prog Neurobiol* **2018**, *171*, 32–49. https://doi.org/10.1016/j.pneurobio.2018.10.001.

APPENDIX

Appendix 1 – List of Taqman mRNA probes used in this study

Protein	Gene
GluA1	GRIA1
TARPy-8	cacng8
PSD-95	dlg4
GAPDH	gapdh

Appendix 2 – List of primary antibodies used in this study

Antibody	Dilution Factor	Molecular Weight (kDa)	Host (Mouse or Rabbit)
pGluA1-Ser831	1:3,000	106	R
TARPy-8	1:8,000	50	R
PSD-95	1:500,000	95	M
GAPDH	1:10,000	37	M